Inhibition of iron corrosion in high temperature stagnant liquid lead: A molecular dynamics study

Artoto Arkundato [a,*], Zaki Su'ud [b], Mikrajuddin Abdullah [b], Widayani Sutrisno [b], Massimo Celino [c]

[a] Physics Department, Jember University, Jl. Kalimantan 37, Jember, Indonesia
[b] Physics Department, Bandung Institute of Technology, Jl. Ganesha 10, Bandung, Indonesia
[c] ENEA, CR Casaccia, Via Anguillarese 301, Rome, Italy

ABSTRACT

Corrosion property of iron in high temperature stagnant liquid lead has been studied using molecular dynamics method. The method was used to predict the limit values of the injected oxygen into the liquid lead for maximum corrosion inhibition of iron. It is from experimental results, in order to inhibit the corrosion at possible lowest rate then a stable self-healing protective iron oxide layer should be developed at the surface of steel continuously. In this research we investigated the iron corrosion and it can be predicted that the protective oxide layer may be formed by injecting oxygen within the range of 5.35×10^{-2} wt% to 8.95×10^{-2} wt% (for observed temperature 750 °C). The oxygen 5.35×10^{-2} wt% is the lower limit to prevent high dissolution of iron while the oxygen content of 8.95×10^{-2} wt% is the upper limit to avoid high precipitation of lead oxide. We also guess that effect of oxygen injection into liquid lead creates a thin oxygen barrier that separating the liquid lead and iron oxides from direct interaction. The iron oxides layer and oxygen barrier then may be regarded as double corrosion inhibition.

© 2013 Elsevier Ltd. All rights reserved.

1. Introduction

For design of fast nuclear reactors, lead (Pb) is one of popular coolant material candidates (Zhang and Li, 2008). Liquid lead has boiling temperature 1740 °C which is above the melting temperature of reactor clad, and also has relatively low melting point 327 °C (Bentor and Yinon, 2013). Lead is also chemically inert with respect to water compared with the sodium. Lead has also high thermal conductivity compared with water. Those physical and chemical properties determine margins of its operation region in reactor application (Sobolev, 2007). However, it is well known that the cladding and structural materials are severely corroded if they are exposed to high temperature liquid lead directly. The dissolution of steel components under high temperature liquid lead is very high (Kashezhev et al., 2010; Zelenskii et al., 2007; Zhang et al., 2010; Zhang and Li, 2008). High dissolution of iron in liquid lead causes destruction (corrosion) of iron (Manly, 1959). The corrosion exactly has limited the lifetime of reactor operation, and this crucial problem has presented a critical challenge in application of liquid lead for design of fast reactor. We need to know a way for inhibiting strong corrosion of liquid lead or developing corrosion-resistant novel materials, not only under normal condition but also in temporary anomalous condition (Rivai and Takahashi, 2010).

Although many experiments about liquid lead/lead alloys corrosion have been reported, however a fully understanding how to manage the corrosion are still not completed, yet. In addition, not all experiments may or easy be done within an operating reactor. In this situation then simulation methods have become a promising technique for studying corrosion. However, the number of publications about simulation of corrosion phenomena of liquid lead is still few, especially using molecular dynamics (MD) simulation method. Maulana et al. (2008) in their preliminary work had studied the penetration depth of atoms of liquid lead into Fe–Ni–Cr steel by using the Lennard-Jones (LJ) MD simulation. However they did not explore the thermodynamics properties of the corrosion such as the diffusion coefficient and also did not study the corrosion inhibition mechanism. In the previous work (Arkundato et al., 2010) we had applied the MD simulation method to calculate the diffusion coefficient of iron in stagnant liquid lead. In the current work we study corrosion inhibition. To realize the simulations we used the MOLDY MD program that is a powerful technique for material computation (Ackland et al., 2011; Refson, 2000).

A technique of reducing the corrosion is to develop a stable self-healing protective oxide layers on the surface of structural materials (cladding, pipe, vessel system, etc.) to prevent direct high dissolution of metal components. This protective layer may be developed by maintaining the dissolved oxygen into liquid lead (Bolind, 2009; Rivai and Takahashi, 2010; Zelenskii et al., 2007; Zhang et al., 2010; Zhang and Li, 2008). This protective oxide layers cut down the dissolution rate of material components of the

* Corresponding author. Tel.: +62 331 334293; fax: +62 331 330225.
E-mail address: a.arkundato@gmail.com (A. Arkundato).

structural materials toward liquid lead, since the material components must first pass through the oxides (Bolind, 2009). An active oxygen control with suitable concentration in liquid lead can bring to the acceptable low corrosion rates and to prevent the precipitation of lead oxides in the liquid lead. Experiments show the optimum oxygen concentration was controlled within the range of magnetite (Fe_3O_4) and PbO oxide formation (Doubkova et al., 2006).

In our previous preliminary work (Arkundato et al., 2012) we also have used the LJ MD simulation to study the effect of oxygen injection to reduce the corrosion rate of pure iron. However at that work we could not show the upper limit value of the oxygen content for development of stable protective oxide layer, yet. It is from experiments the oxygen content for injection has two limit values (Doubkova et al., 2006). We also had not explored the structure of iron in liquid lead for different oxygen concentrations completely. Soontrapa and Chen have successfully used the Embedded Atomic Method (EAM) potential for MD simulation to model the iron oxidation during magnetite development (Soontrapa and Chen, 2009). However they did not study the corrosion based on the coefficient diffusion calculation as we did in our work, yet. Moreover, they did not explore the effect of oxygen for different contents in reducing the corrosion to predict the minimum and maximum threshold values of the oxygen content. The purpose of the current research is to study the mechanism of corrosion inhibition and to predict the minimum and maximum limit values of oxygen content for development of a continuous stable protective oxide layer for effective corrosion inhibition. We model the corrosion of pure iron in liquid lead for preliminary study. The reason why we choose the iron as a study is to compare the simulation results with available experimental data (Zhang and Li, 2008). For corrosion inhibition we used oxygen injected into liquid lead with the oxygen potential parameter as reported by Lemmon and Jacobsen (2004) and included more atoms in the simulation (10745 Fe and 45006 Pb).

2. Theoretical background

2.1. Molecular dynamics method

Molecular dynamics method is a simulation technique in which atoms of material under investigation is allowed to evolve for a specified period of time, an inter-atomic potential and a certain simulation condition (temperature, pressure, density, etc.), creating trajectories of atoms. In MD simulation the forces have to be specified. Denoting f_{ij} is the force exerted by atom j on atom i then the total force acting on atom i is

$$\vec{F}_i = \sum_j \vec{f}_{ij} \tag{1}$$

In this equation, $\vec{F}_i$ is the total force experienced by atom i due to all other atoms j in the studied material system. If the force is conservative, the force is equal to negative gradient of potential energy $u(\vec{r})$ i.e.

$$\vec{f} = -\nabla u(\vec{r}) \tag{2}$$

The Eq. (1) may be written as

$$\vec{F}_i = -\nabla \sum_j u_{ij}(\vec{r}_{ij}) \tag{3}$$

Then dynamics motion of the system can be governed by the Newton equation:

$$m_i\{d^2\vec{r}_i/dt^2\} = \vec{F}_i \tag{4}$$

r_i is the position of atom i. Generally the material system is a complex one, then the Newton equation needs to be solved numerically. One of the popular techniques for solving the equation is the

Modified Beeman algorithm that we also used in this research (Refson, 2000). In our work we used the MOLDY MD program, the one that can perform simulation of many phases of material (solids, liquids and gas) (Refson, 2000).

2.2. Interatomic potential

In this preliminary work we used the Lennard-Jones (n–m) potential for simplifying the study. We used the Lennard-Jones potential parameters that derived by Zhen and Davies (1983) based experimental measurement. The general Lennard-Jones potential is (Zhen and Davies, 1983),

$$u(r) = k\varepsilon\lfloor(\sigma/r)^n - (\sigma/r)^m\rfloor \tag{5}$$

where σ and ε are the LJ potential parameters. The k is a coefficient to specify the LJ potential function,

$$k = \frac{n}{n-m}\left(\frac{n}{m}\right)^{m/(n-m)} \tag{6}$$

Especially if we take values $n = 12$ and $m = 6$, we have the popular LJ potential,

$$u(r) = 4\varepsilon\lfloor(\sigma/r)^{12} - (\sigma/r)^6\rfloor \tag{7}$$

The (12-6) LJ potential is simple physical model of interaction that approximates the interaction between a pair of neutral atoms. To simplify simulations as a preliminary study, we used the LJ potential. The interaction potential of Fe–Fe and Pb–Pb is supported by potential parameters as reported by Zhen and Davies (1983) based on his experimental data. For O–O interaction we used potential parameter as reported by Lemmon and Jacobsen (2004). The cross-interactions (Fe–Pb, Fe–O and Pb–O) are generated by the popular Lorentz–Berthelot mixing rule (Brodholt and Wood, 1993):

$$\sigma_{AB} = (\sigma_{AA} + \sigma_{BB})/2 \tag{8}$$

$$\varepsilon_{AB} = \sqrt{(\varepsilon_{AA} \times \varepsilon_{BB})} \tag{9}$$

Table 1 summarizes the LJ potential parameters that used in our simulation.

2.3. Diffusion and corrosion in high temperature condition

Corrosion of steels may be defined as a structural degradation into its constituent atoms. The solubility of its components (Fe, Cr and Ni, etc.) plays an important role in corrosion phenomena when using heavy liquid metals as the lead (Bolind, 2009; Manly, 1959; Zhang and Li, 2008). Temperature is an important factor of corrosion because the higher temperature of liquid metal (coolant) the higher solubility of steel components. The temperature of liquid lead is increased then the diffusion rate of the steel components will be increased, with the result that high corrosion of the steels. In operating of nuclear reactor, the fission reactions in the fuel inside the cladding produce heat that creates high temperature of coolant. This high temperature condition creates high corrosion condition of the structural material of reactor. Generally

Table 1
Table of LJ potential parameters

Pair interaction	σ (Å)	ε (eV)
Fe–Fe	0.4007	2.3193
Pb–Pb	0.1910	3.1888
O–O	0.0102	3.4280
Fe–Pb	0.2766	2.7541
Fe–O	0.0639	2.8737
Pb–O	0.0441	3.3084

the corrosion is chemical process. But Manly (1959) have stated that the corrosion of steel in high temperature liquid metals has a strong contribution from non-chemical actions, in which no transfer of electrons is observed. The corrosion is effect of high dissolution of steel components in liquid metals. So, in this preliminary work we make approach that we can focus on the physical process (mechanical features) of corrosion and not to chemical reaction contributions.

To simplify corrosion study we model the corrosion of pure iron (major component of steel). We prepare simulation by placing the bcc pure iron (box) in the centre of the liquid lead, simulate the system with certain high temperature and then analyze the result of simulation. From the trajectories of the atomics motion after simulation then we calculated the diffusion coefficient Eq. (11) to investigate the iron corrosion. The diffusion calculation needs the mean square displacement (MSD) calculations Eq. (10) as a part of Einstein relation for D coefficient. The temperature dependence of diffusion coefficient $D(T)$ can be calculated by using the popular Arrhenius formula Eq. (12). Those three important equations are (Kupryazhkin et al., 2008):

$$MSD = \langle |\vec{R}(t) - \vec{R}(0)|^2 \rangle \tag{10}$$

$$D = \lim_{t \to \infty} MSD/6t \tag{11}$$

$$D(T) = D_0 \exp(-A/\Re T) \tag{12}$$

where t is time, T is temperature, A is activation energy for corrosion to be happen and $\Re$ is a gas constant. To know the structure properties of materials before and after inhibition we calculate the radial distribution function (RDF), $g(r)$ and also observe the stability of the iron structure using the common neighbor analysis (CNA). CNA calculation is performed by OVITO code (Stukowski, 2010). To know the microscopic structure of iron before and after simulations we plot the coordinate xyz of atoms by using Jmol visualization code (Hanson, 2010).

3. Simulation procedure and details

The study of iron corrosion and its inhibition are described as below procedure:

(I) Model of iron, liquid lead and model of corrosion. In this step we need to check the phase stability of the material model. The model should be checked by considering the melting point of the material. We placed box of bcc iron in the centre of liquid lead (Fig. 1).
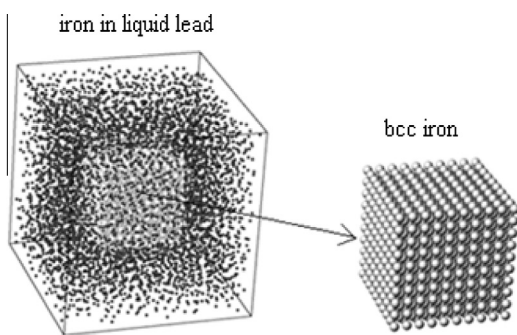
(II) Check the equilibration condition of simulation.

(III) Simulation of iron corrosion in liquid lead at several elevated high temperatures within the range of 600–1100 °C to calculate the diffusion coefficient of iron $D(T)$ by using Eq. (12).

(IV) Comparison of the obtained diffusion coefficients with available experimental data as reported by Zhang and Li (2008). This is to check a validity of the simulation corrosion model.

(V) Simulation of oxygen injection into liquid lead (based on the above model) to study corrosion inhibition, at temperature 750 °C. Oxygen will be injected with several small different concentrations (wt%).

(VI) Calculate the MSD, RDF (by MOLDY code), the diffusion coefficient $D(T)$ and CNA number (by Ovito code) and observe the microscopic structure of iron (by Jmol code). Analyse what concentration the oxygen will reduce the corrosion rate significantly and efficiently.

3.1. Step I, II, III

The simulation model was prepared in a simulation box where the iron bulk (1729 Fe atoms in $9 \times 9 \times 9$ bcc crystal unit with lattice constant $a = 2.8286$ Å) was placed in the centre of the liquid lead (consist of 5577 Pb atoms with atomic density 0.0274 atoms/Å³). The simulation box had dimension $63.2 \times 63.2 \times 63.2$ Å³. The iron-lead system was simulated for elevated temperatures: 600 °C, 650 °C, 700 °C, 750 °C, 800 °C, 850 °C, 900 °C, 950 °C, 1000 °C, and 1050 °C. The parameters of simulation control in the Moldy input are: the NPT ensemble Anderson mode, zero pressure, Nose-Hoover thermostat and 0.0001 ps of time size. The numerical integration was carried out by using the modified Beeman integration (Refson, 2000). The equilibration condition was achieved after 2.0 ps of integration (see Fig. 2), and average of properties calculation was done for duration of 10 ps.

3.1.1. Phase stability

The phase stability of the simulation model is important. In this way we need to simulate pure iron without interaction with liquid lead. We simulate from lower temperature (where the melting temperature of the lead is) till high enough temperature (where the melting temperature of iron is). The melting temperature of the lead is about 327 °C and the melting temperature of iron is about 1538 °C (Bentor and Yinon, 2013). At temperature 327 °C, by this simulation model, the iron should be confirmed in the solid phase and at temperature 1538 °C should be in liquid phase. We can check this phase condition by plotting the MSD curves. The solid phase will be represented by approximately horizontal curve and the liquid phase will have linear line with a big angle from horizontal axis. We can see the stability of iron by checking this MSD curves. If we can see that for lower temperatures (327 °C and
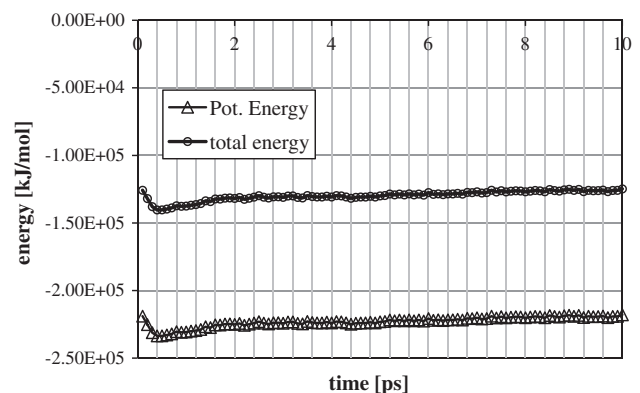

Fig. 1. Iron material with a bcc crystal structure placed in the centre of liquid lead

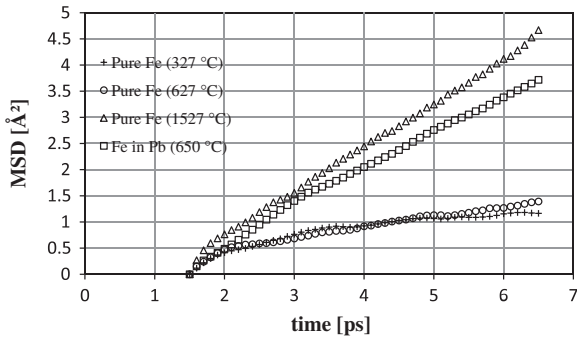**Fig. 2.** Equilibration curve of Fe-Pb simulation

Fig. 3. MSD curves of pure iron with interaction and without interaction with lead

627 °C for examples) the iron still in the solid phases, then we believe that the LJ potential model is approximately correct.

Then we need to simulate the iron with interaction with molten lead, where this should effect high corrosion of iron. Thus, we put the iron within molten lead at certain temperature where we want to study the corrosion that is about 650 °C. At this condition there are high dissolution of Fe atoms, the iron will go to the melting phase. The MSD curve of iron will show a characteristic of liquid. Even the temperature of study (∼650 °C) is still far from the melting temperature of iron (∼1527 °C), the iron should be confirmed to experience high corrosion from simulation result. It is from our simulation that all the above assumption is relatively correct as Fig. 3. From this figure we have conclusion that at temperature about 650 °C the isolated iron is still in crystalline state, on the contrary within molten lead the iron is not in the crystalline trend (MSD has big angle). Then we concluded that our model of LJ potential is relatively correct with certain degree of accurate. We have proved that Fe is a reliable crystalline material in the temperature range we are interested in. This is all we need to perform our simulations.

3.1.2. Melting point

The information of melting point of Pb and Fe from simulation may be very important in this study. However in our study we are only interested to make sure that at temperature (∼600 °C) the iron model is in the solid phase (without interaction with liquid lead) because this is far from melting temperature (∼1527 °C). And we also interested to make sure that at temperature about 327 °C, the phase of molten lead is liquid because this is the melting point of the lead. Then we study the iron corrosion within molten lead at the temperature about 600 °C to up, where the experimental data is available (Zhang and Li, 2008) for compare. Fig. 4 is the RDF function of molten lead at 650 °C.
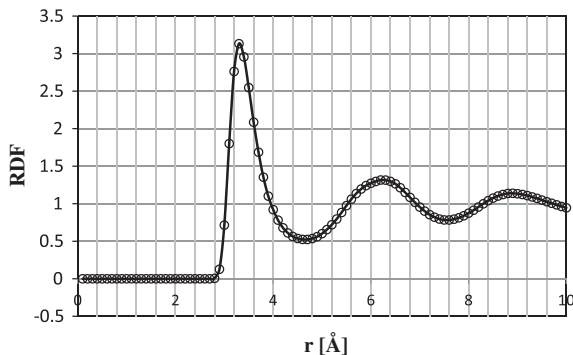
3.2. Step IV

To study the effect of oxygen injection for iron corrosion inhibition, we enlarged our iron-lead system and added oxygen for certain small concentrations. We enlarged the corrosion system because of following the experiment results that oxygen content in the liquid lead should be in a very small amount that may about 10^{-2} wt% compared with the liquid lead weight (Zelenskii et al., 2007). Now our simulation is the iron-oxygen-lead system, which has dimension of $(123 \times 123 \times 123)\,\text{Å}^3$ where the iron bcc bulk is still placed in the centre of the system whereas oxygen atoms is inserted and distributed evenly in the molten lead with certain small wt%. By remembering that the oxygen molecules (O_2) should undergo ionization at high temperature then in our model of corrosion inhibition we regarded that the oxygen atoms are as separated atoms and will be distributed evenly in the molten lead. In this classical molecular dynamics study we also regarded that the oxygen atoms are neutral atoms. We just consider the mechanical process of corrosion by observing the diffusion. We are not studying the chemical process of corrosion. From this work we have shown that the oxygen injection if one of mechanism of corrosion inhibition of iron in molten lead. We agree with reviewer that this study should be continued for better investigation. It is for the next research. Thus O–O interatomic model is not a crucial element of our model. This is confirmed by the overall good agreement with experimental results our numerical model.

The current number of iron atom is 10745 and the lead is 40685 of Pb atoms. We have several iron-lead-oxygen simulations for same temperature (750 °C) but with different oxygen contents: 340 atoms (0.0583 wt%), 450 atoms (0.0771 wt%), 674 atoms (0.1152 wt%), 906 atoms (0.1552 wt%), 1132 atoms (0.1938 wt%) and 1348 atoms (0.2307 wt%). The consideration of using fixed single temperature 750 °C is to compare our results with available experimental data that have been reported by Zhang and Li (2008). This is also to accommodate the abnormal condition of fast reactor during accident, where it can reach very high temperature, about 750 °C. At this step of simulation, from analysis of simulation results, it should be able to predict the proper oxygen content for significant and effective iron-corrosion inhibition.

4. Results and discussions

4.1. Iron diffusion coefficient without oxygen injection

After completing step I, II, III of simulation, we calculated MSD, D and $D(T)$ by using Eqs. (10)–(12). Fig. 5 is a plot of $\log D$ vs. $1/T$ for
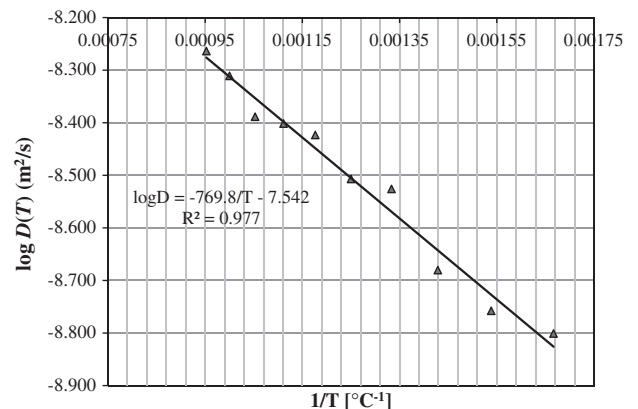

Fig. 4. RDF curve of molten lead at temperature 650 °C

$\log D = -769.8/T - 7.542$
$R^2 = 0.977$

Fig. 5. Plot of $1/T$ and $\log D$ from simulations of iron in liquid lead

iron diffusion. The line in Fig. 5 has mathematical expression as following:

$$\log D(T) = -769.814/T - 7.542 \quad (13)$$

Using Eqs. (11) and (12) then we can predict the temperature dependence of iron diffusion is:

$$D_{0.00wt\%}(T) = 2.865 \times 10^{-8} \cdot \exp(\{-1764.971 \pm 94.436\}/T) \\ \times (m^2/s) \quad (14)$$

Now we calculate the coefficient diffusion of iron for temperature 750 °C, following Eq. (14):

$$D(T = 750°C) = (2.723 \pm 0.344) \times 10^{-9} (m^2/s) \quad (15)$$

Robertson had reported the experimental results, that the iron diffusion in pure liquid lead was $D_{Fe \to Pb} = 2.80 \times 10^{-9}$ m²/s for temperature 750 °C (Zhang and Li, 2008). Comparing our MD result Eq. (15) with Robertson's result then there is an agreement to about 99.22%. Furthermore Balbauer-Celerier and Barbier have used a correlation for lead that was developed by Robertson, and they proposed that the iron diffusion coefficient in liquid lead could be approached by (let's say BCBR curve) (Zhang and Li, 2008):

$$D_{Fe \to Pb}(T) = 4.9 \times 10^{-7} \cdot \exp(\{-44100 \pm 6300\}/\Re T) \quad (16)$$

Following the BCBR curve Eq. (16), the iron diffusion coefficient in liquid lead is in the range of $(1.31–5.75) \times 10^{-9}$ m²/s at temperature 750 °C. Our MD calculation Eq. (15) then is in a good agreement to the BCBR result Eq. (16) for temperature 750 °C. Fig. 6 shows a comparison between our MD calculation Eq. (15) and BCBR experimental result Eq. (16). From Fig. 6 we can see that our model of corrosion simulation may be applied to study liquid lead corrosion for temperatures about 750 °C downward.

4.2. Effect of oxygen injection

The inhibition of iron corrosion in liquid lead was achieved by injecting the oxygen atoms into liquid lead. Effect of oxygen injection can be seen in Fig. 7. The smaller corrosion rate is described by lower MSD line. From that figure, we see a small concentration of oxygen injection has effect of lowering the MSD line. If the diffusion rate depend on the MSD then the corrosion rate also depend on the MSD. Then an injection of oxygen to the liquid lead has push down the corrosion rate. The RDF function can show the phase of material. RDF calculations can be done by using MOLDY easily. The RDF profile can give information about material phase. Solid material have the RDF peaks tend in the form of high sharp modes. Liquid material have the RDF peaks tend in the form of low smooth modes. Fig. 8 shows the RDF profiles of iron diffusion for different
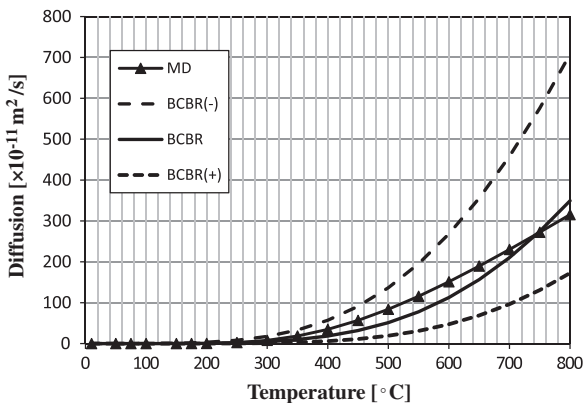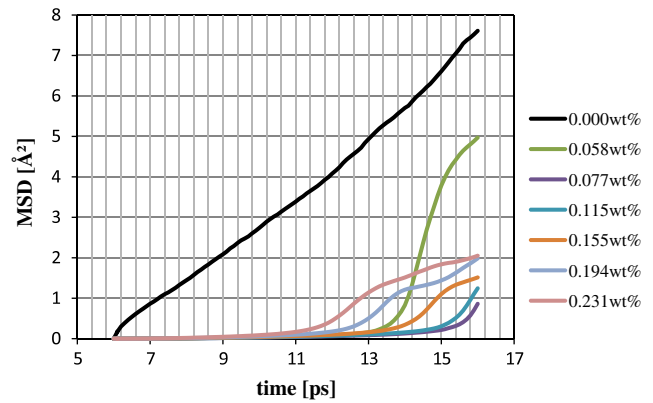

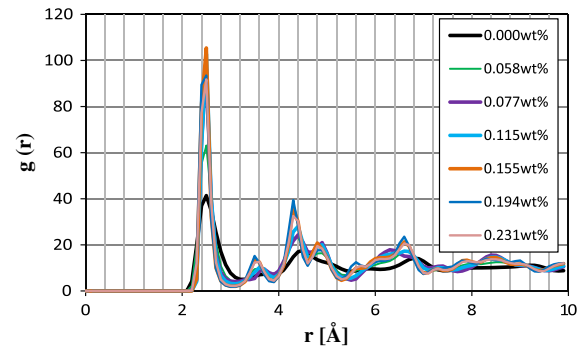**Fig. 7.** MSD curves of iron in liquid lead with difference oxygen contents

Fig. 8. RDF curves of iron in liquid lead with difference oxygen contents
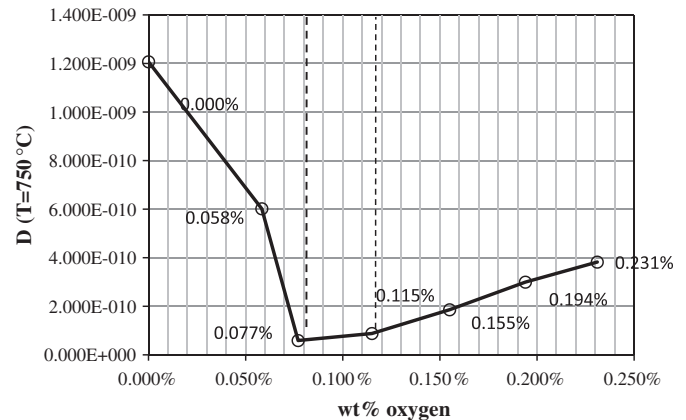

Fig. 9. Effect of oxygen injection for corrosion inhibition profile

oxygen concentrations. Injecting the oxygen for only small percentage has maintained the iron material in the form of solid phase (RDF curve with high sharp peaks). The RDF curves of Fig. 8 can give descriptions of phases of iron (in high temperature liquid lead) for different oxygen contents. For normal condition without oxygen injection the iron material has been brought to the non-solid phase condition (forced melting) as a result of high dissolution of iron at high temperature (black curve). By injection of oxygen the characteristic of RDF curves shows the trend of solid phase condition (other curves).

A clear picture of effect of oxygen injection for corrosion inhibition is in Fig. 9. If we use Eq. (11) to calculate the diffusion coefficient then we can see that there is a narrow interval of oxygen

Fig. 6. Comparison of diffusion coefficient curve between our calculation and BCBR result

concentration where the injection will effect maximum stable corrosion inhibition. From that Fig. 9 we can see that the injection of 0.0771–0.115 wt% will inhibit the iron corrosion rate significantly at the lowest level. At this interval of oxygen concentration the corrosion rate is also stable minimum. From Fig. 9 then we have three pictures of corrosion areas: (1) the oxygen injection below 0.0771 wt% where the corrosion is still high (by dissolution of Fe atoms), (2) the oxygen injection between 0.0771 wt% and 0.115 wt% where there is maximum stable corrosion inhibition and very low corrosion rate and (3) the oxygen injection more than 0.115 wt% where high corrosion rises again. The injection of oxygen below 0.0771 wt% is not enough to protect the iron from attack of high corrosion. In this MD simulation we found that the limit values of oxygen content for maximum corrosion inhibition of iron degradation are 0.0771 wt% for lower limit and 0.115 wt% for upper limit.

Fig. 10a shows a microstructure of iron before simulation, the iron bcc crystal. The microstructure of iron corrosion after 16 ps simulation steps without oxygen issue is shown by Fig. 10b. It can be understood that iron has been highly corroded. The injection of 0.0583 wt% of oxygen is still not enough to protect high corrosion of iron, Fig. 10c. A fascinating picture is shown by Fig. 10d and e where after injecting oxygen for content of 0.0771 wt% and 0.155 wt%, the corrosion of iron has been significantly reduced. Fig. 10f–h are the microstructures of iron after injection for more than 0.115 wt%, which show that the corrosion has been promoted again.

4.3. Review on the oxide formation

Molten liquid lead is aggressive to the structural material due to high solubility of material components (such as Fe, Ni and Cr). Injection of oxygen into liquid lead is regarded to be able to protect the steel from high dissolution by forming of protective oxide scales/layers/films on the metal surfaces (Bolind, 2009; Rivai and Takahashi, 2010; Zhang and Li, 2008). The range of possible oxygen contents is regulated by the necessity to establish a protective oxide scale and to avoid liquid metal oxides precipitation (Doubkova et al., 2006). From our MD simulation we have predicted that the range of possible oxygen contents is between two limit values 0.0771 wt% and 0.115 wt%. From Fig. 9 we have seen that the degradation of iron was decreased drastically in this possible range. The stable protective oxide film will be developed by about 0.0771 wt% oxygen injection. This stability of lowest corrosion rate of iron can still be maintained until the upper limit of injection 0.115 wt%. In this way, a useful range of oxygen contents in a system containing liquid lead has been advised, that is defining a lower limit (0.0771 wt%) where the development of iron oxide has been guaranteed and an upper limit (0.115 wt%) where a precipitation of lead oxide will appear. Actually, inside this range of two values, the protectiveness of the oxides can vary in function of the structural material composition (Doubkova et al., 2006). In general from experiments, the lower limit for the oxygen content is defined by the formation of stable protective oxides, should be magnetite oxides (Fe_3O_4) in this iron case, while the higher limit (upper limit)
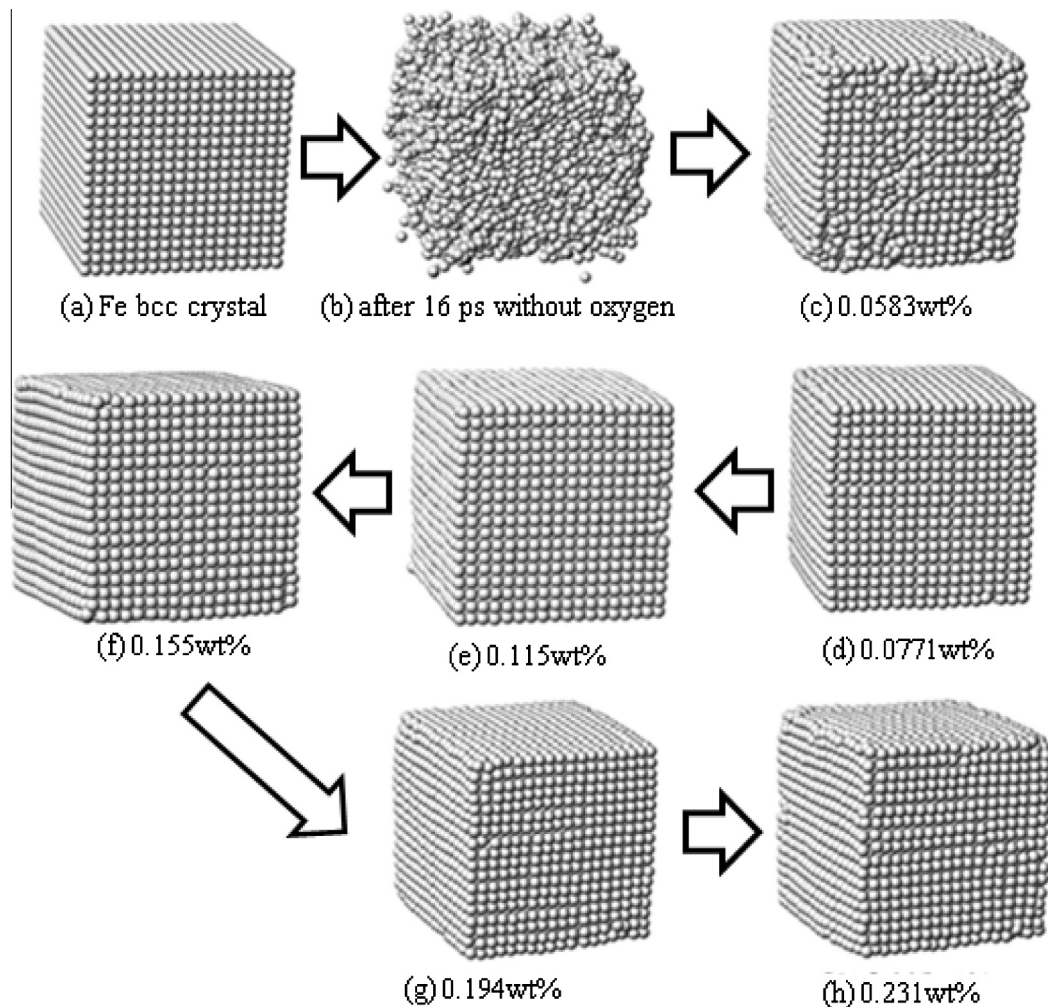

Fig. 10. Microstructure views of iron with difference oxygen contents in liquid lead

is established by initiation of precipitation of lead oxide, for example PbO (Doubkova et al, 2006). From thermodynamics point of view the lower limit of oxygen content provide a sufficient potential to develop a stable magnetite layer on the material (Doubkova et al., 2006). This can be evaluated from the Ellingham diagram that plots the free energy of oxides formation and temperatures (Martinelli et al., 2008). For deeper analysis of oxides formation it is better to calculate the Ellingham diagram and this need more simulation data. This is not done in this current research yet and will be done in future research. The precipitation of liquid metal oxides is not desirable and the main oxide formed in liquid lead should be lead monoxide (PbO) in this iron case (Doubkova, 2006; OECD/NEA Handbook, 2007).

Now let's discuss and examine the microscopic views of iron, liquid lead and oxygen from simulation results. Fig. 11a shows that without oxygen injection then Pb atoms near the surface of iron will interact strongly with Fe atoms of iron surfaces. Many Pb atoms can penetrate the surface of iron causing high degradation (corrosion). However, injecting only 0.0583 wt% of oxygen into liquid lead has reduced the lead attacks (Fig. 11b). Some oxygen atoms enter the surface of the iron. From experimental point of view these oxygen atoms at the surface section of the iron *starts to develop iron oxide layer* to maintain the bcc structure of iron from lead attacks. This injection 0.0583 wt% of oxygen still cannot inhibit the corrosion perfectly. The structure iron at surface has still experienced degradation. The injection of oxygen in the range of 0.0771–0.115 wt% seems to be able to develop a stable iron oxide layers to protect the bcc structure of iron continuously (Fig. 11c and d). However, increasing the oxygen for more than 0.155 wt%

seems to promote corrosion (Fig. 11e–g) again. From that Fig. 11e–g we see the structure of iron at surface section start to change and experience next degradation. From experimental point of view this due to precipitation of process of lead oxides. More oxygen injected more precipitation take places. Fig. 10 has shown this condition clearly. Moreover is also from Fig. 11b then we propose there is a very narrow space filled by some oxygen atoms that separating the liquid lead and iron oxides. This narrow space then may be regarded as a barrier for double protection from corrosion. The first protection is iron oxides the second protection is oxygen barrier. Off course if possible, this second conclusion (oxygen barrier) should be checked experimentally.

At this step we have three important points: (1) the oxygen injected will support for developing the stable self-healing protective iron oxide layer for corrosion inhibition (Zhang and Li, 2008), (2) this oxide layer may be develop by injecting oxygen in the range of 0.0771 wt% to 0.115 wt% and (3) we guessed the injected oxygen atoms also create a thin barrier that trying to separate the liquid lead and iron.

4.4. Relation between oxygen content and simulation time

It is necessary to check the oxygen content for corrosion inhibition as long as the simulation done. We want to check whether the injected oxygen at start of simulation is still same as the last simulation for corrosion inhibition. In our previous conclusion we have found that the maximum corrosion inhibition of iron in liquid lead can be maintain if we inject the oxygen in the range of 0.0771–0.115 wt%. Actually these two values of oxygen content are the
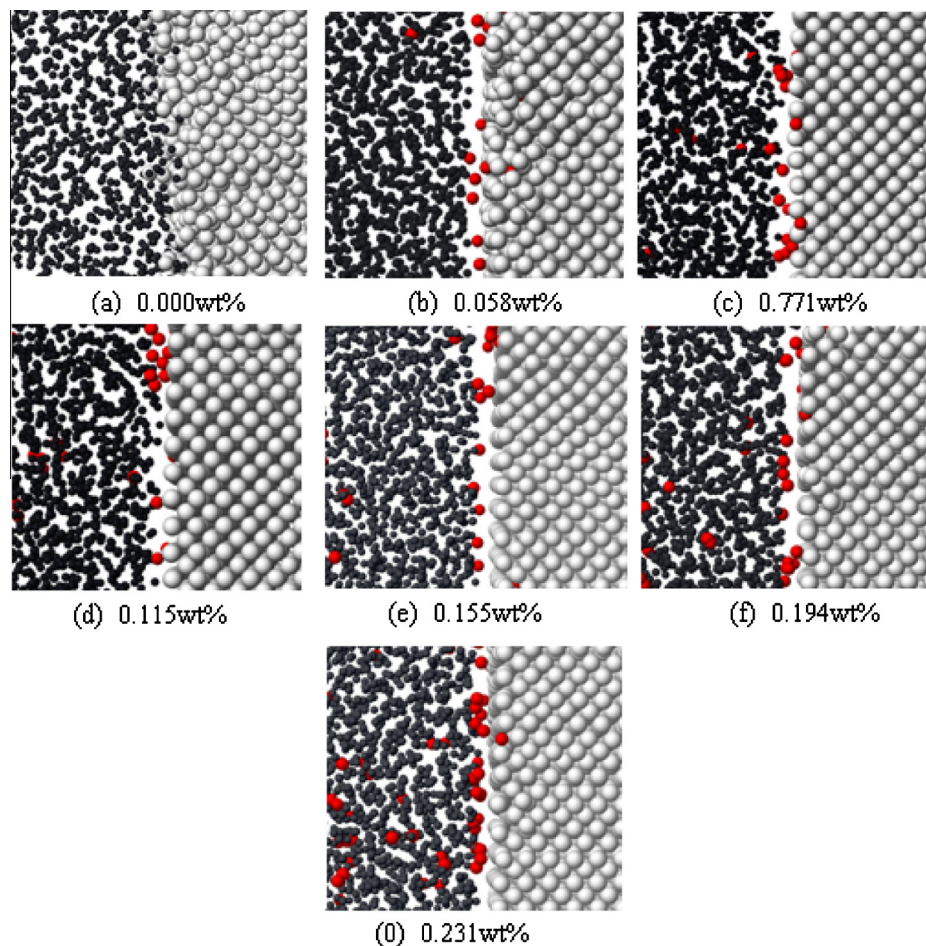

Fig. 11. Microscopic views of iron, lead and oxygen atoms at the corrosion area
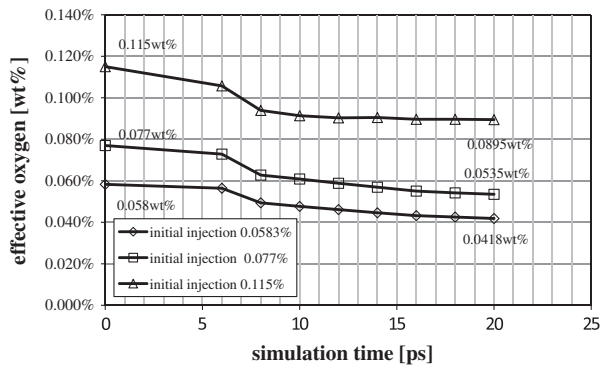
Fig. 12. The effective oxygen contents for iron corrosion inhibition in liquid lead

oxygen atoms that we give to MD simulation input. In the MD simulation method the studied system should be equilibrated for some times to achieve equilibration condition. We found from the simulation that after 20 ps not all of oxygen atoms will be used to maintain the maximum corrosion inhibition. Some of oxygen atoms will be at the outside of lead liquid after the system experiences an equilibrium condition. The most part of oxygen atoms (effective number) are still in liquid lead to support the development of oxygen barrier and oxides. Fig. 12 shows the effective oxygen contents in lead liquid after 20 ps simulation. We can see after 8 ps simulation, the needed oxygen atoms for corrosion inhibition go to stability. We can see for 0.0771 wt% of oxygen injection at start of simulation, after 20 ps the iron-lead system only need 0.0535 wt% of oxygen for effective corrosion inhibition. For 0.155 wt% of oxygen injection at start of simulation, we only need 0.0895 wt%. The oxygen contents 0.0535 wt% and 0.08952 wt% are the oxygen atoms those are still in the corroded system. The rest of oxygen atoms have gone to the outside of corroded system after equilibrium process of the simulated system.

Based in Fig. 12 then we make important correction that for developing a stable self-healing protective oxide layer for maximum corrosion inhibition and also to support the forming of oxygen thin barrier to separate the liquid lead and iron then we need to maintain the oxygen injection in the range of 0.0535–0.0895 wt%.

4.5. Comparison with experimental results

The following discussion then is the comparison between our MD results with experimental results. There is an experimental result about the EP823 steel corrosion in liquid lead. The corrosion inhibition was studied by injecting the oxygen at the level of about 10^{-3} wt% at 700 °C. Zelenskii et al. (2006, 2007) also studied the 15Kh12MS2AG steel in lead liquid at 750 °C and using the oxygen injection of 1.9×10^{-2} wt% to reduce the corrosion. Lead oxide PbO was introduced into the lead to ensure constant oxygen content in lead during the test at the level of 1.9×10^{-2} wt%. After some testing, they found an oxide that will prevent high corrosion process of steels. In our study we used the iron, not novel steel as usually used in advanced experimental works. However our results confirmed that the high corrosion of iron can be reduced by oxygen injection for content of about 0.0535 wt% or 5.353×10^{-2} wt%.

4.6. Structure analysis of corroded iron with CNA method

Figs. 10b and 11a shows that before oxygen injection the atomic structure of iron is highly destructed when iron placed in the liquid lead at high temperature 750 °C. Then, after oxygen injection the iron structure show sas a more ordered system like a crystal structure. Actually we need to check that after corrosion inhibition by
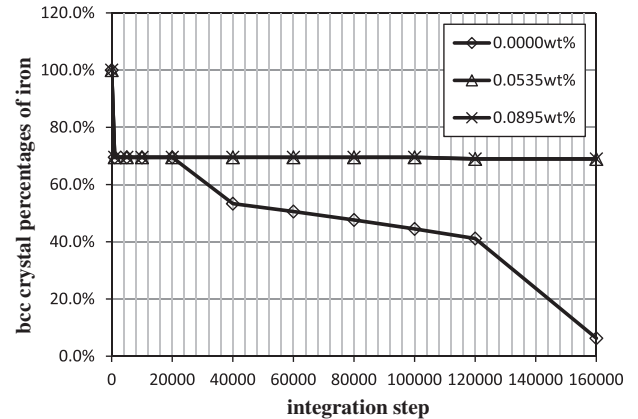

Fig. 13. CNA calculation for iron in liquid lead with proper oxygen injection

oxygen injection whether all Fe atoms of iron will be in the form of bcc crystal structure or not. The CNA (common neighbor analysis) method can give description of structure stability of material such as iron from corrosion attack while the oxygen atoms are injected into liquid lead. By knowing the coordinates (positions) of iron atoms we can calculate how many atoms are arranged in bcc crystal or fcc or hcp lattice or others. In this work the CNA calculation was done by OVITO code (Stukowski, 2010). Fig. 13 shows the result of CNA calculation.

It can be seen that the effect of oxygen injection 0.0535 wt% and 0.0895 wt% will maintain the bcc structure of iron, be spared from continuous degradation via high dissolution of Fe atom in high temperature liquid lead. It can be seen the oxygen injection will maintain about 70% atoms of iron material still in the form of bcc crystal structure. This is different from the case of without oxygen injection (0.0000 wt% curve) where after the 20,000 integration step the bcc crystal structure of iron material have been destructed rapidly and after long time integration the bcc structure will be totally destructed.

5. Conclusions

By molecular dynamics simulation we can calculate that the diffusion coefficient of iron in liquid lead is $D(T) = 2.865 \times 10^{-8} \cdot \exp(\{-1764.971 \pm 94.436\}/T)$. For maximum corrosion inhibition of iron we can inject the proper oxygen content for about 5.35×10^{-02} wt% to 8.95 10^{-2} wt% into the liquid lead for development of stable self-healing protective oxide layer in the surface of iron material. This oxygen injection is capable to maintain the iron with 70% of its Fe atoms still in the form bcc crystal structure. The injected oxygen atoms will be used to develop a stable self-healing protective oxide layer in the surface of iron material to prevent iron corrosion. We also guess that the effect of oxygen injection will also create a thin oxygen barrier that separating the liquid lead and iron material. The iron oxide layer and thin oxygen barrier will support double corrosion inhibition.

References

Arkundato, A., Su'ud, Z., Mikrajuddin, A., 2010. Corrosion study of Fe in a stagnant liquid Pb by molecular dynamics methods. AIP Conf. Proc. 1244, 136–144.

Arkundato, A., Su'ud, Z., Mikrajuddin, A., Widayani, S., Massimo, C., 2012. Numerical study: iron corrosion-resistance in lead-bismuth eutectic coolant by molecular dynamics method. AIP Conf. Proc. 1454, 65.

Ackland, G.J., D'Mellow, K., Daraszewicz, S.L., Hepburn, D.J., Uhrin, M.K., Stratford, 2011. The MOLDY short-range molecular dynamics package. Comp. Phys. Commun. 182, 2587.

Bentor, Yinon, (2013), Chemical Element.com – Lead. <http://www.chemicalelements.com/elements/pb.html> (accessed on 21.03.13).

Bolind, A. M., 2009, PhD Thesis, Nuclear Engineering, University of Illinois at Urbana-Champaign, Urbana, Illinois, USA.

Brodholt, J., Wood, B., 1993. Molecular dynamics simulations of the properties of CO_2–H_2O mixtures at high pressures and temperatures. Am. Mineral. 78, 558.

Doubkova A., Karnik, D., Di Gabriele, F., 2006, The influence of the oxygen content on the metal loss of the austenitic steel 17246 (AISI 321) in flowing liquid lead-bismuth eutectic. <http://nuklearserver.ka.fzk.de/OFMS/Web%2fMain%2fPublications%2f2006%2fDEMETRA%2fP_A.Doubkova_ JournNuclMat_2006.pdf> (accessed on 01.06.012).

Hanson, R.M., 2010. Jmol – a paradigm shift in crystallographic visualization. J. Appl. Crystallogr. 43 (5), 1250–1260. http://dx.doi.org/10.1107/S0021889810030256.

Kashezhev, A.Z., Ponegev, M.Kh., Sozaev, V.A., Khasanov, A.I., Mozgovo, A.G., 2010. An experimental investigation of the wetting of reactor steels with molten lead and bismuth. High Temp. 48 (5), 756.

Kupryazhkin, A.Y., Zhiganov, A.N., Risovany, D.V., Nekrassov, K.A., Golovanov, V.N., 2008. Simulation of diffusion of oxygen and uranium in uranium dioxide nanocrystals. J. Nucl. Mater. 372, 233.

Lemmon, E.W., Jacobsen, R.T., 2004. Viscosity and thermal conductivity equations for nitrogen, oxygen, argon. Inter. J. Thermophysics 25 (1), 21.

Maulana, A., Su'ud, Z., Hermawan, K.D., Khairurrijal, 2008. Simulation study of steels corrosion phenomenon in liquid lead-bismuth cooled reactors using molecular dynamics methods. Prog. Nucl. Energy 50, 616–620.

Manly, W.D., 1959, Fundamentals of liquid–metal corrosion. >http://www.ornl.gov/info/reports/1956/3445603500959.pdf> (accessed on March 2013).

Martinelli, L., Balbaud-Célérier, F., Picard, G., Santarini, G., 2008. Oxidation mechanism of a Fe–9Cr–1Mo steel by liquid Pb–Bi eutectic alloy (Part III). Corros. Sci. 50, 2549–2559.

OECD/NEA Handbook on lead-bismuth eutectic alloy and lead properties, materials compatibility, thermal hydraulics and technologies Nuclear Energy Agency 2007. <http://www.oecd-nea.org/science/reports/2007/pdf/chapter4.pdf>. (accessed on 21.03.12)

Refson, K., 2000. Moldy: a portable molecular dynamics simulation program for successive and parallel computers. Comp. Phys. Commun. 126 (3), 309–328.

Rivai, A.K., Takahashi, M., 2010. Corrosion characteristics of materials in Pb–Bi under transient temperature conditions. J. Nucl Mater. 398, 139.

Sobolev, V., 2007. Thermophysical properties of lead and lead bismuth eutectic. J. Nucl. Mater. 362, 235.

Soontrapa, C., Chen, Y., 2009. Optimization approach in variable-charge potential for metal/metal oxide systems. Comput. Mater. Sci. 46 (4), 887.

Stukowski, A., 2010. Visualization and analysis of atomistic simulation data with OVITO – the Open Visualization Tool. Simul. Mater. Sci. Eng., 18.

Zhen, S., Davies, G.J., 1983. *L-J n–m* potential energy parameters: calculation of the LJ n–m pot energy parameters for metals. Phys. Stat. Sol. (a) 78, 595.

Zelenskii, G.K., Ivanov, Y.A., Ioltukhovskii, A.G., Naumenko, I.A., Shkabura, I.A., 2006. Possible ways for protecting fuel claddings from corrosion on the side of the heat-transfer lead sublayer. Metal Sci. Heat Treat. 48, 412.

Zelenskii, G.K., Ioltukhovskii, A.G., Leont'eva-Smirnova, M.V., Naumenko, I.A., Tolkachenko, S.A., 2007. Corrosion resistance of fuel element steel cladding in a lead coolant. Metal Sci. Heat Treat. 49 (11–12), 533–538.

Zhang, J., Li, N., 2008. Review of the studies on fundamental issues in LBE. J. Nulc. Mater. 373, 351–377.

Zhang, V., Hosemann, P., Maloy, S., 2010. Models of liquid metal corrosion. J. Nucl. Mater. 404, 82.